

# Spin Glass Behavior in $\text{RuSr}_2\text{Gd}_{1.5}\text{Ce}_{0.5}\text{Cu}_2\text{O}_{10}$

C. A. Cardoso\*, F. M. Araújo-Moreira

Grupo de Materiais e Dispositivos, CMM-C, Departamento de Física, UFSCar, Caixa Postal 676, 13565-905, São Carlos-SP, Brazil

V. P. S. Awana, E. Takayama-Muromachi

Superconducting Materials Center (Namiki Site), National Institute for Materials Science, 1-1 Namiki, Tsukuba, Ibaraki 305-0044, Japan

O. F. de Lima

Instituto de Física "Gleb Wataghin", UNICAMP, 13083-970, Campinas-SP, Brazil

H. Yamachi, M. Karppinen

Materials Science Laboratory, Tokyo Institute of Technology, Nagatsuta 226-8503, Yokohama, Japan  
(Sept 24, 2002)

The dynamics of the magnetic properties of polycrystalline  $\text{RuSr}_2\text{Gd}_{1.5}\text{Ce}_{0.5}\text{Cu}_2\text{O}_{10}$  (Ru-1222) have been studied by ac susceptibility and dc magnetization measurements, including relaxation and ageing studies. Ru-1222 is a reported magneto-superconductor with Ru spins magnetic ordering at temperatures near 100 K and superconductivity in Cu-O<sub>2</sub> planes below  $T_c \approx 40$  K. The exact nature of Ru spins magnetic ordering is still debated and no conclusion has been reached yet. In this work, a frequency-dependent cusp was observed in  $\chi_{ac}$  vs.  $T$  measurements, which is interpreted as a spin glass transition. The change in the cusp position with frequency follows the Vogel-Fulcher law, which is commonly accepted to describe a spin glass with magnetically interacting clusters. Such interpretation is supported by thermomagnetic magnetization (TRM) measurements at  $T = 60$  K. TRM relaxations are well described by a stretched exponential relation, and present significant ageing effects.

The coexistence of superconductivity and magnetic order in ruthenium copper oxides  $\text{RuSr}_2(\text{Gd};\text{Sm};\text{Eu})_2\text{Cu}_2\text{O}_{10}$  (Ru-1222)<sup>1,16</sup> and  $\text{RuSr}_2(\text{Gd};\text{Sm};\text{Eu})\text{Cu}_2\text{O}_{10}$  (Ru-1212) has attracted a lot of attention recently<sup>7,19</sup>. But, besides this considerable interest, there are yet some unresolved questions about the exact type of magnetic order in these compounds. The difficulty about understanding the magnetic ordering in these systems is that different techniques like muon spin rotation (SR)<sup>9</sup>, magnetic resonance (MR)<sup>12</sup>, neutron powder diffraction (NPD)<sup>13;16,18</sup>, magnetization<sup>14;19</sup> and nuclear magnetic resonance (NMR)<sup>15</sup>, though indicate towards canted antiferromagnetic ordering with a ferromagnetic component, they do not agree completely with each other. Although ferromagnetism and antiferromagnetism seem to be competing in these compounds<sup>13;16,18</sup>, nobody speculates about the possibility of this competition to cause a frustration of the spin system, leading to a spin-glass scenario. The situation is especially unclear for the Ru-1222 family. For Ru-1222, though NPD results were reported recently<sup>20</sup>, the magnetic structure has not been unveiled. Although the magnetic behavior of Ru-1222 has been considered to be analogous to the magnetic response for Ru-1212 samples, some recent results point towards various differences<sup>3</sup>.

In this work we explore the magnetic behavior of poly-

crystalline Ru-1222 samples by ac susceptibility ( $\chi_{ac} = \chi' + i\chi''$ ), dc magnetization, and resistivity measurements. We observe a significant dependence of  $\chi_{ac}$  on the frequency of the excitation field  $h = h_0 \sin(\omega t)$ , which is characteristic of spin glass systems. The temperature shift of the cusp in  $\chi''$  follows the Vogel-Fulcher law, which describes the freezing temperature  $T_f$  of spin glasses with magnetically interacting clusters. Such interpretation is consistent with the observation of stretched exponential relaxations and the occurrence of ageing effects at temperatures below the magnetic ordering temperature.

## I. EXPERIMENTAL DETAILS

The  $\text{RuSr}_2\text{Gd}_{1.5}\text{Ce}_{0.5}\text{Cu}_2\text{O}_{10}$  (Ru-1222) sample was synthesized through a solid-state reaction route from  $\text{RuO}_2$ ,  $\text{SrO}_2$ ,  $\text{Gd}_2\text{O}_3$ ,  $\text{CeO}_2$ , and  $\text{CuO}$ . Calcinations were carried out on the mixed powder at 1000, 1020, 1040, and 1060 °C each for 24 hours with intermediate grindings. The pressed bar-shaped pellets were annealed in a flow of high-pressure oxygen (100 atm) at 420 °C for 100 hours and subsequently cooled slowly to room temperature<sup>21</sup>. X-ray diffraction (XRD) patterns were obtained at room temperature (MAC Science: MXP 18 VHF<sup>22</sup>; CuK $\alpha$  radiation). Resistivity measurements

were made in the temperature range of 5 to 300 K using a four-point-probe technique. All ac susceptibility measurements were performed in a commercial PPM S (Physical Properties Measurement System), while for the dc measurements a SQUID magnetometer MPM S-5 were employed, both equipments made by Quantum Design company.

## II. RESULTS AND DISCUSSION

Presently studied, Ru-1222 copper oxide sample crystallizes in a tetragonal structure of space group  $I4mm$  with  $a = b = 3.8327(7)$  Å and  $c = 27.3926(8)$  Å. The X-ray diffraction pattern, Fig. 1, shows a single phase material, without any detectable impurity peak. The compound exhibited superconductivity ( $R = 0$ ) below 40 K in electrical transport measurements<sup>21</sup>, as shown in the inset of Fig. 1. To recall the characteristic magnetic behavior of Ru-1222; Fig. 2 displays the temperature dependence of both zero field cooled (ZFC) and field cooled (FC) dc magnetization measured at  $H = 50$  Oe. The ZFC branch presents a pronounced peak at  $T_p = 68$  K, just below the temperature where the ZFC and FC curves separated. The freezing temperature  $T_f$ ; extracted from ac susceptibility measurements, is also indicated and will be discussed later. At  $T_c = 45$  K is observed a kink in both ZFC/FC curves as the Ru-1222 goes through its superconducting transition. The steady increase of the FC branch at low temperatures is interpreted as being caused by the paramagnetic response of the Gd ions. It is important to notice that some magnetic ordering starts to occur at a temperature  $T = 160$  K much higher than  $T_p$ . This can be observed in the inset of Fig. 2, which shows an enlarged view of the magnetization curve at temperatures above  $T_p$  revealing a small hysteresis at these temperatures. Interestingly, both curves merge together again at a temperature around 80 K. The anomaly observed at  $T$  was previously reported as associated with an antiferromagnetic transition<sup>5</sup>, possibly in analogy to the magnetic ordering occurring in Ru-1212: In the same temperature region we observed a small bump in  $T$  measurements (not shown). We speculate if this anomaly could indicate the appearance of spin clusters which at a lower temperature would have the magnetic moments frozen to originate a spin-glass system. In Fig. 3 we present a magnetization curve measured as a function of field,  $M(H)$ . The magnetization does not saturate even at the highest field 90 kOe, as shown in the inset of Fig. 3, which is consistent with what is expected for a spin-glass. The low field portion of the virgin branch of the hysteresis loop at 60 K displays an S shape, with a positive curvature at low fields, a typical characteristic of spin-glass systems. It is important to notice that  $T = 60$  K  $\gg T_c = 45$  K, thus this positive curvature at low field is not due to a superconductor contribution superimposed with a magnetic

loop. Another striking characteristic of the virgin branch is that it stays outside the hysteresis loop. This unusual behavior was previously reported for cluster glasses with magnetic interacting clusters<sup>22,24</sup>. It seems to be related with the more common displaced loop observed when the sample is field cooled<sup>22,23;25;26</sup>, though a more recent work consider it should be due to a strong increase of the local surface anisotropy when the sample is cooled below a certain characteristic temperature, for a system of nanosized antiferromagnetic particles in an amorphous matrix<sup>24</sup>.

The ac susceptibility ( $\chi_{ac}$ ) technique is a very powerful method to provide evidence of a spin-glass behavior. In this case, both components  $\chi'$  and  $\chi''$  of  $\chi_{ac}$  present a sharp, frequency dependent cusp. The position of the cusp in  $\chi'$  denotes the freezing temperature  $T_f$ , which is coincident with the temperature of the inflection point in  $\chi''$ . It is also well known that dc magnetic fields as low as a few hundreds of Oersted can round this cusp up. In Fig. 4 we present the ac susceptibility for our sample measured at  $H_{dc} = 50$  Oe. The main frame of Fig. 4 presents the ZFC/FC temperature dependence of both  $\chi'$  and  $\chi''$  for the frequency  $\nu = 10000$  Hz.  $\chi'$  presents a sharp drop at the superconducting transition temperature  $T_c$  and a sharp, frequency dependent peak at  $T_f = 72$  K. The peak shifts to lower temperatures and its intensity increases as the frequency of the excitation field is decreased (see upper inset, Fig. 4). For the  $\chi''$  peak we observe the shift to lower temperatures as well as a decrease of its intensity with decreasing frequency (see lower inset of Fig. 4). The frequency dependence of both components is a typical feature of the dynamics of spin-glass systems. The coincidence of the temperature of both, the peak in  $\chi'$  and the inflection point in the  $\chi''$  curve, is also verified in our data. The  $\chi'$  component presents a double anomaly in the 110–170 K range, but neither frequency nor thermal magnetic history dependences are observed. The imaginary component does not present any significant feature in this temperature range. On the other hand, for temperatures below 60 K a clear separation of the ZFC/FC curves is observed in both components, although it is more prominent in  $\chi''$ .

To further verify the existence of a spin-glass behavior, we have studied the frequency dependence of  $\chi_{ac}$  in more detail. A quantitative measure of the frequency shift is obtained from  $T_f = [T_f \log(\nu)]$ . This quantity varies in the range of 0.004–0.018 for spin-glass systems<sup>27</sup>, while for superparamagnets<sup>27</sup> it is of the order of 0.3. From a set of FC susceptibility measurements at different frequencies, presented in the upper inset of Fig. 4, we could estimate  $T_f = [T_f \log(\nu)] = 0.005$  for our Ru-1222 sample. Therefore, our data are consistent with the spin-glass hypothesis. There are basically two different possible interpretations of the spin-glass freezing: the first one assumes the existence of a true equilibrium phase transition at a finite temperature (canonical spin glasses)<sup>28</sup>. The second interpretation assumes the existence of clusters and, in this case, the freezing

is a nonequilibrium phenomenon<sup>29</sup>. For isolated clusters (superparamagnets), the frequency dependence of their freezing temperature (in this context more correctly referred as blocking temperature) has been predicted to follow an Arrhenius law

$$\tau = \tau_0 \exp[ E_a/k_B T_f ]; \quad (1)$$

where  $E_a$  is the potential barrier which separates two easy orientations of the cluster and  $\tau$  is the driving frequency of the ac measurement. However, for magnetically interacting clusters, a Vogel-Fulcher law has been proposed:

$$\tau = \tau_0 \exp[ E_a/k_B (T_f - T_0) ]; \quad (2)$$

where  $T_0$  can be viewed as a phenomenological parameter which describes the intercluster interactions. Equation 2 implies a linear dependence of the freezing temperature with  $1/\ln(\tau_0^{-1})$ ;  $\tau_0 = 1/\ln(\tau_0^{-1}) = 2/\ln(\tau_0^{-1})$ . In Fig. 5 we present a Vogel-Fulcher plot, which shows that our data follow the expected linear behavior. From the best linear fit we obtained  $\tau_0 = 10^{12}$  Hz,  $T_0 = 66.92$  K and  $E_a = 76.92$  K.

Also, the existence of the spin-glass behavior has been checked through the time-dependent magnetic behavior of our sample. In this case, thermomagnetic magnetization (TRM) measurements were performed. Since the behavior of a spin glass below  $T_f$  is irreversible and complicated by ageing processes, it is imperative to employ a well-defined H-T cycling procedure to obtain meaningful data. The precise procedure adopted in this work to measure the TRM relaxation was the following: the sample was field cooled (H = 5000 Oe) down from 200 K to 60 K; after temperature stabilization we waited for a certain time  $t_w$ . Thereafter the field was reduced to zero and the magnetization was recorded as a function of the elapsed time. The results for different values of  $t_w$  ( $100 < t_w < 1000$  s) are presented in Fig. 6. Among the various functional forms that have been proposed to describe the magnetic relaxation in spin glasses, one of the most popular is the so-called stretched exponential

$$M(t) = M_0 - M_\infty \exp \left[ - \left( \frac{t}{t_p} \right)^n \right]; \quad (3)$$

where  $M_0$  relates to an intrinsic ferromagnetic component and  $M_\infty$  to a glassy component mainly contributing to the relaxation effects observed. Both  $M_\infty$  and  $t_p$  (the time constant) depend upon  $T$  and  $t_w$ , while  $n$  is only a function of  $T$ . If  $n = 0$  one has the Debye, single time-constant, exponential relaxation. On the other hand, for  $n = 1$ , one does not have any relaxation at all. The solid lines in Fig. 6 are the best fits of equation 3 to our experimental data, with parameters  $4.38 \cdot 10^3 < M_0 < 4.49 \cdot 10^3$  emu,  $3.3 \cdot 10^4 < M_\infty < 3.7 \cdot 10^4$  emu, and  $n = 0.45$  (fixed for all fittings). The single parameter which presents a large variation with changes in the wait

time is the time constant  $t_p$ , which goes from  $t_p = 1749$  s for  $t_w = 100$  s to  $t_p = 5214$  s for  $t_w = 1000$  s. The changes observed in  $M(t)$  measured for different values of  $t_w$  demonstrate the occurrence of ageing effects, what means that the physical system is in a metastable state. In the inset in Fig. 7 this point is emphasized by showing the relaxation rate  $S(t) = -dM/d \ln(t)$ . The shift in the minimum position of  $S(t)$ ; expected to occur for a spin-glass system, is clearly observed.

### III. CONCLUDING REMARKS

The frequency-dependent peak observed in the temperature dependence of the ac susceptibility  $\chi_{ac}$ , combined with magnetic relaxation results, provides strong evidence of the important role of magnetic frustration in polycrystalline Ru-1222 to establish the existence of cluster glass properties over a significant temperature range. This is to be contrasted with the usual interpretation of the existence of long-range antiferromagnetic order with spin canting for both Ru-1222 and Ru-1212 samples. The microscopic reason why Ru-1212 may present a long-range order while Ru-1222 does not is not clear at this time. However, our results come in line with the recent findings of Zivkovic et al., Ref. 3, who have pointed out significant differences in the magnetic behavior of these two families of ruthenocuprates. Also, their results indicate the existence of a metastable magnetic state below the magnetic transition at  $T_f$ , which is in agreement with our interpretation of a cluster glass freezing at  $T_f$ .

### IV. ACKNOWLEDGMENTS

We thank L.M. Socolovsky for fruitful discussions. This work was supported by Brazilian agencies Fundao de Amparo a Pesquisa do Estado de So Paulo (FAPESP) through contracts # 95/4721-4, 01/05349-4, and Conselho Nacional de Pesquisas (CNPq) through contract # 300465/88-2.

---

\*Electronic address: cardoso@dfufscar.br

<sup>1</sup> I. Felner, U. A. Saf, Y. Levi, and O. M. Ilbo, Phys. Rev. B 55, R 3374 (1997).

<sup>2</sup> I. Felner and U. A. Saf, Int. J. Mod. Phys. B 12, 3220 (1998)

<sup>3</sup> I. Zivkovic, Y. Hirai, B. H. Frazer, M. P. Prester, D. Drobac, D. A. Riosa, H. Berger, D. Pavuna, G. M. Argarito, I. Felner, and M. O. Nellion, Phys. Rev. B 65, 144420 (2002).

<sup>4</sup> Y. Hirai, I. Zivkovic, B. H. Frazer, A. Reginelli, L. Perfetti, D. A. Riosa, G. M. Argarito, M. P. Prester, D. Drobac, D. T. Jiang, Y. H. Hu, T. K. Sham, I. Felner, M. Pederson, and M. O. Nellion, Phys. Rev. B 65, 054417 (2002).

- <sup>5</sup> M. T. Escote, V. A. Maza, R. F. Jardim, L. Ben-Dor, M. S. Torikachvili, and A. H. Lacerda, to appear in Phys. Rev. B.
- <sup>6</sup> V. P. S. Awana, S. Ichihara, M. Karppinen, and H. Yamachi, Physica C 378-381, 249 (2002).
- <sup>7</sup> V. P. S. Awana, S. Ichihara, J. Nakamura, M. Karppinen, H. Yamachi, J. Yang, W. B. Yelon, W. J. James, and S. K. Malik, J. Appl. Phys. 91, 8501 (2002).
- <sup>8</sup> X. H. Chen, Z. Sun, K. Q. Wang, S. Y. Li, Y. M. Xiong, M. Yu, and L. Z. Cao, Phys. Rev. B 63, 064506 (2001).
- <sup>9</sup> C. Bernhard, J. L. Tallon, Ch. Niedermayer, Th. Blassius, A. Golnik, E. Brucher, R. K. Kramer, D. R. Noakes, C. E. Stronack, E. J. Snakdo, Phys. Rev. B 59, 14099 (1999).
- <sup>10</sup> J. L. Tallon, C. Bernhard, M. E. Bowden, T. M. Soto, B. Walker, P. W. Gilberd, M. R. Presland, J. P. Attfield, A. C. Mclaughlin, and A. N. Fitch, IEEE J. Appl. Supercond. 9, 1696 (1999).
- <sup>11</sup> D. J. Pingle, J. L. Tallon, B. G. Walker, and H. J. Tordahl, Phys. Rev. B 59, R11679 (1999).
- <sup>12</sup> A. Fainstein, E. Winkler, A. Butera, and J. Tallon, Phys. Rev. B 60, R12597 (1999).
- <sup>13</sup> J. W. Lynn, B. Kramer, C. Ulrich, C. Bernhard, and J. L. Tallon, Phys. Rev. B 61, R14964 (2000).
- <sup>14</sup> G. V. M. Williams and S. Kramer, Phys. Rev. B 62, 4132 (2000).
- <sup>15</sup> Y. Tokunaga, H. Kotegawa, K. Ishida, Y. Kitaoka, H. Takagiwa, and J. Akimitsu, Phys. Rev. Lett. 86, 5767 (2001).
- <sup>16</sup> H. Takagiwa, J. Akimitsu, H. Kawano-Furukawa, and H. Yoshizawa, J. Phys. Soc. Japan 70, 333 (2001).
- <sup>17</sup> O. Chmaissem, J. D. Jorgensen, H. Shaked, P. Dolar, and J. L. Tallon, Phys. Rev. B 61, 7401 (2000).
- <sup>18</sup> J. D. Jorgensen, O. Chmaissem, H. Shaked, S. Short, P. W. Klamut, B. Dabrowski, and J. L. Tallon, Phys. Rev. B 63, 054440 (2001).
- <sup>19</sup> A. Butera, A. Fainstein, E. Winkler, and J. Tallon, Phys. Rev. B 63, 054442 (2001).
- <sup>20</sup> C. S. Kneee, B. D. Reinford, and M. T. Weller, J. Mater. Chem. 10, 2445 (2000).
- <sup>21</sup> V. P. S. Awana, M. Karppinen, H. Yamachi, R. S. Liu, J. M. Chen and L.-Y. Jang, to appear in J. Low Temp. Phys. (2002).
- <sup>22</sup> P. A. Beck, Progr. Mater. Science 23, 1 (1978).
- <sup>23</sup> R. W. Knitter, J. S. Kouvel, and H. Claus, J. Magn. Mater. 5, 356 (1977).
- <sup>24</sup> R. D. Zysler, D. Fiorani, and A. M. Testa, J. Magn. Mater. 224, 5 (2001).
- <sup>25</sup> C. M. Hurd, Contemp. Phys. 23, 469 (1982).
- <sup>26</sup> P. J. Ford, Contemp. Phys. 23, 141 (1982).
- <sup>27</sup> Spin glasses: an experimental introduction, J. A. Mydosh (Taylor & Francis, London, 1993).
- <sup>28</sup> E. A. Edwards, and P. W. Anderson, J. Phys. F 5, 965 (1975).
- <sup>29</sup> J. L. Tholence, and R. Tournier, J. Phys. (Paris) Colloq. 35, C4-229 (1974).

FIG. 1. Powder x-ray diffraction pattern for Ru-1222 sample. Inset:  $R(T)$  measurement at  $H = 0$  showing the superconducting transition.

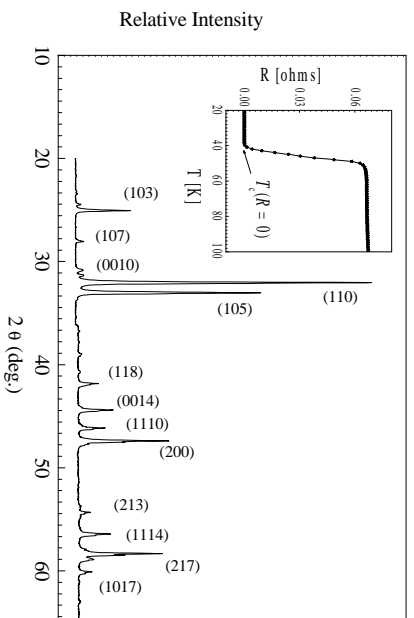
FIG. 2. Field cooled and zero field cooled temperature dependence of magnetization for  $H = 50$  Oe. Inset: amplification of the  $M(T)$  curves showing the small hysteresis at high temperatures.

FIG. 3. Low field portion of the  $M(H)$  curve at  $T = 60$  K. Inset: entire  $M(H)$  curve for fields up to 90 kOe.

FIG. 4. Complex susceptibility as a function of temperature for  $\omega = 10$  kHz (main panel). Upper (lower) inset shows the frequency dependence of the peak in the real (imaginary) component at the freezing temperature  $T_f$ .

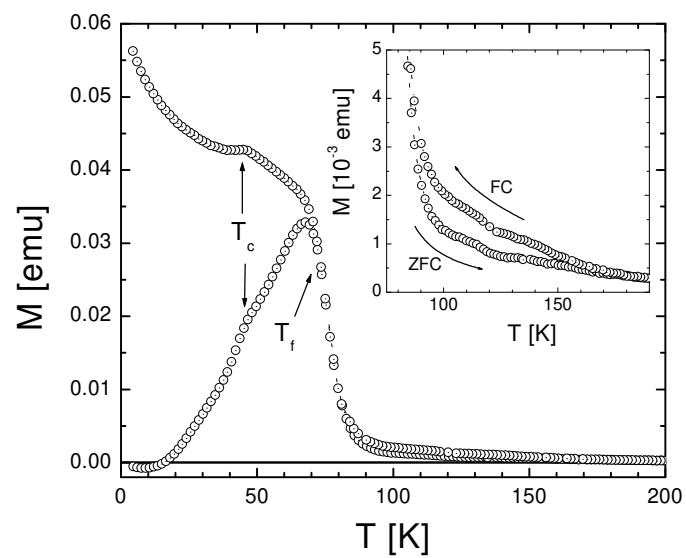
FIG. 5. Variation of the freezing temperature  $T_f$  with the frequency of the ac field in a Vogel-Fulcher plot. The solid line is the best fit of Eq. 2.

FIG. 6. Thermomagnetic magnetization relaxation for  $T = 60$  K and  $t_w = 100$  s (squares); 500 s (circles), and 1000 s (triangles). The solid lines are the best fits of Eq. 3. Inset: relaxation rate  $S(t) = -dM/d \ln(t)$  for the relaxations presented in the main panel.



Cardoso et al. - Fig. 1

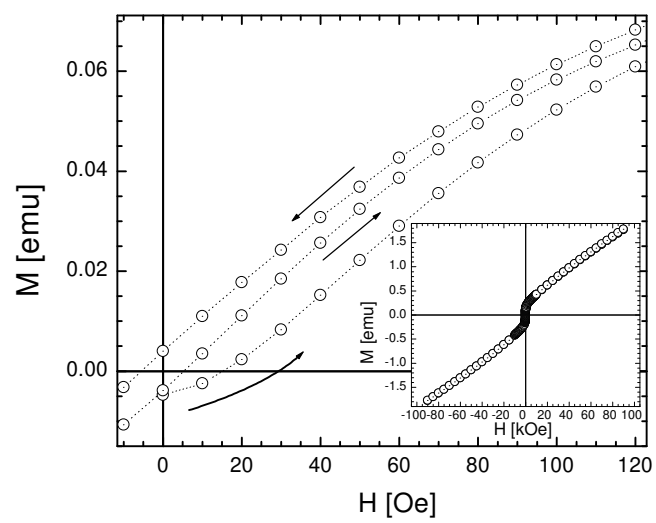




Cardoso et al. - Fig. 2

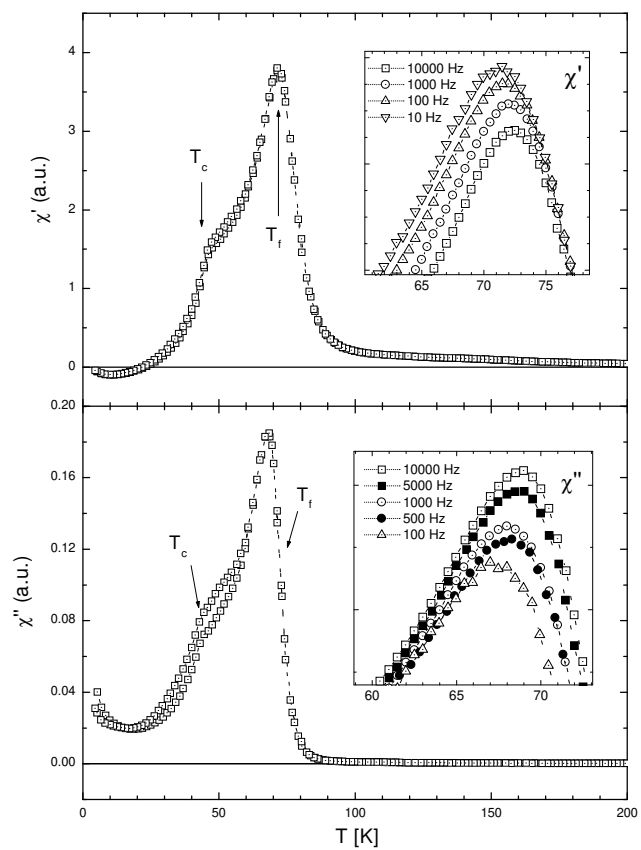






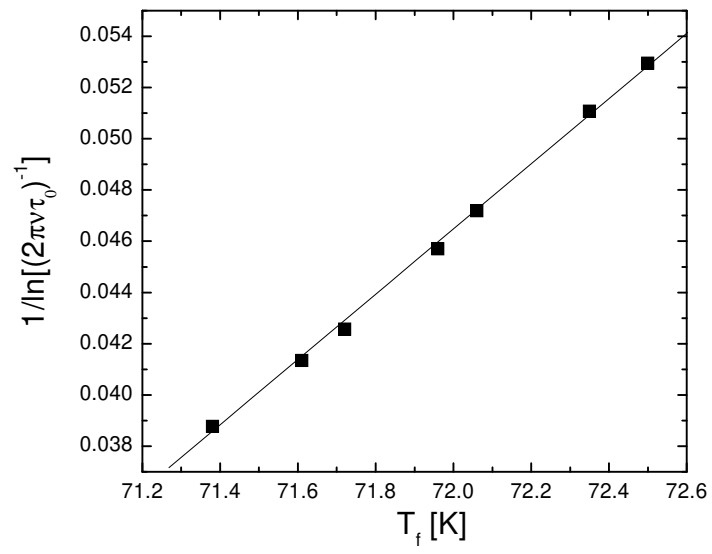
Cardoso et al. - Fig. 3





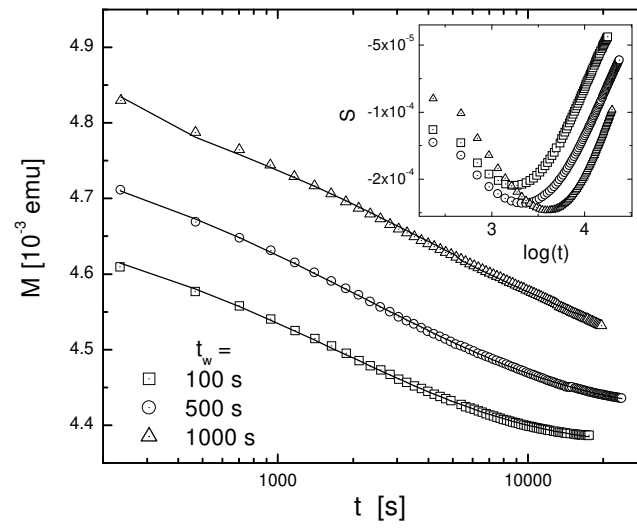
Cardoso et al. - Fig. 4





Cardoso et al. - Fig. 5





Cardoso et al. - Fig. 6

